

Is sea-ice-driven Eurasian cooling too weak in models?

James A. Screen¹ and Russell Blackport¹

ARISING FROM M. Mori et al. *Nature Climate Change* <https://doi.org/10.1038/s41558-018-0379-3> (2019)

In a recent Letter, Mori et al.¹ examined connections in observations and climate models between reduced Arctic sea ice and the ‘warm Arctic and cold Eurasia’ (WACE) pattern. They concluded that models systemically underestimate Eurasian cooling in response to sea-ice loss, relative to observations. If correct, their result implies that up to half of the observed Eurasian cooling from 1995–2014 is attributable to sea-ice loss¹, whereas previous studies have found a negligible contribution from sea-ice loss^{2–4}. Here, we highlight that their comparisons between observations and models are not like-for-like, and show that when fair comparisons are made, modelled and observed estimates are consistent with each other. The upward adjustment of the contribution of sea-ice loss to observed Eurasian cooling in Mori et al.¹ is therefore unjustified.

An essential first step in model evaluation is to derive an observational benchmark against which models can be assessed. Mori et al.¹ seek an observational estimate of the WACE response to Barents–Kara sea-ice loss. Their approach is to correlate time series of the WACE pattern and Barents–Kara sea ice. They interpret the squared correlation coefficient multiplied by the WACE variance (hereafter $r^2\sigma^2$) as the fraction of WACE variance driven by sea ice. In doing so, they make an assumption about causality. Their apparent justification for this causal inference is that their analysis detects WACE as the main pattern of sea-ice-driven temperature variability. However, the WACE pattern also varies irrespective of sea ice and, as a result, their observed time series of the WACE (EC_{ERA}) contains both variability driven by sea ice and variability not driven by sea ice. It is important to note that even the non-sea-ice-driven component will correlate with Barents–Kara sea ice because a warm Arctic causes reduced sea ice, and vice versa. Sea ice and WACE variability will correlate because the Arctic temperature and sea ice are strongly and physically connected, even if Eurasian temperature is minimally affected by sea ice, as recent work suggests⁵. For the reasons just given, the interpretation of $r^2\sigma^2$ as the fraction of WACE variance driven by sea ice is questionable and, as we will demonstrate, it is probably an overestimation.

Mori et al.¹ also calculate $r^2\sigma^2$ from atmospheric general circulation model (AGCM) experiments in which sea ice is specified. The interaction between ice and the atmosphere is only in one direction in this experimental set-up: the atmospheric response to varying sea ice is represented, but the response of sea ice to atmospheric variation is not. Mori et al.¹ report that the observed $r^2\sigma^2$ value is roughly twice as high as those obtained from seven different AGCMs, leading them to conclude that models systemically underestimate the WACE response to sea-ice loss. However, their comparison between observations and AGCMs is misleading because the observed $r^2\sigma^2$ reflects two-way interactions between sea ice and the atmosphere, rather than the one-way influence of sea ice on the atmosphere in AGCM-derived $r^2\sigma^2$.

Here, we test the extent to which $r^2\sigma^2$ is suppressed by a lack of two-way interactions in AGCM simulations. We first reproduced the results of Mori et al.¹ (with minor methodological differences; see Methods), which confirms that none of the seven AGCMs reproduce the observed $r^2\sigma^2$ (Fig. 1a). It is important to note that this discrepancy is seen in both the winter months collectively (Fig. 1a) and in winter averages (see fig. 4a in Mori et al.¹), which strongly suggests that the origin of the model–observation disparity is not timescale dependent, and justifies our use of monthly averages in what follows. Next, we compared output from an atmosphere–ocean general circulation model (AOGCM) and an AGCM prescribed with sea ice and sea surface temperatures taken from the parent AOGCM (see Methods). The $r^2\sigma^2$ value in the AOGCM experiment is roughly twice as high as that in the AGCM (Fig. 1b), which we attribute to the simulation of two-way atmosphere–ice interaction in the AOGCM not present in the AGCM. The smaller $r^2\sigma^2$ value in AGCMs compared with observations shown originally by Mori et al.¹ and reproduced here in Fig. 1a need not imply model error. Instead, it could be largely explained by the lack of two-way interaction in AGCM experiments and the inability of the $r^2\sigma^2$ method to extract the sea-ice-driven fraction of observed WACE variability. We caution against directly comparing the observed (Fig. 1a) and AOGCM-derived (Fig. 1b) $r^2\sigma^2$ values as they correspond to different climate states. Although the observed $r^2\sigma^2$ is higher than in the AOGCM, this probably reflects greater sea-ice variability (by ~50%; not shown) in the recent past compared with the pre-industrial climate, rather than model error.

We note that the higher $r^2\sigma^2$ value in the AOGCM compared with the AGCM (Fig. 1b) could arise due to one of two reasons: coupling is necessary to simulate the effects of WACE variability on sea ice, or ocean feedbacks amplify the WACE response to sea-ice loss. Regarding the former, coupled models simulate the effects of WACE-related atmospheric circulation variability on Barents–Kara sea ice similarly to the real world⁵. Regarding the latter, it is clear that ocean feedbacks would strengthen the local warming response to sea-ice loss. However, this need not imply any change in Eurasian cooling. Indeed, Deser et al.⁶ showed that ocean coupling enhanced the Arctic warming and atmospheric circulation responses to sea-ice loss, but suppressed Eurasian cooling. Surveying the literature, there is no evidence that coupled models simulate stronger Eurasian cooling in response to sea-ice loss than uncoupled models^{6–10}.

To gain further insight, and building on work by Blackport et al.⁵, we propose a refined approach to estimate the WACE variance driven by sea ice that can be applied equally to observations and AGCMs. We hypothesize that a better estimate can be obtained from the correlation between the WACE and Barents–Kara sea ice in the preceding month, rather than using the contemporaneous correlation. Lead–lag correlation is a common first step in causal discovery

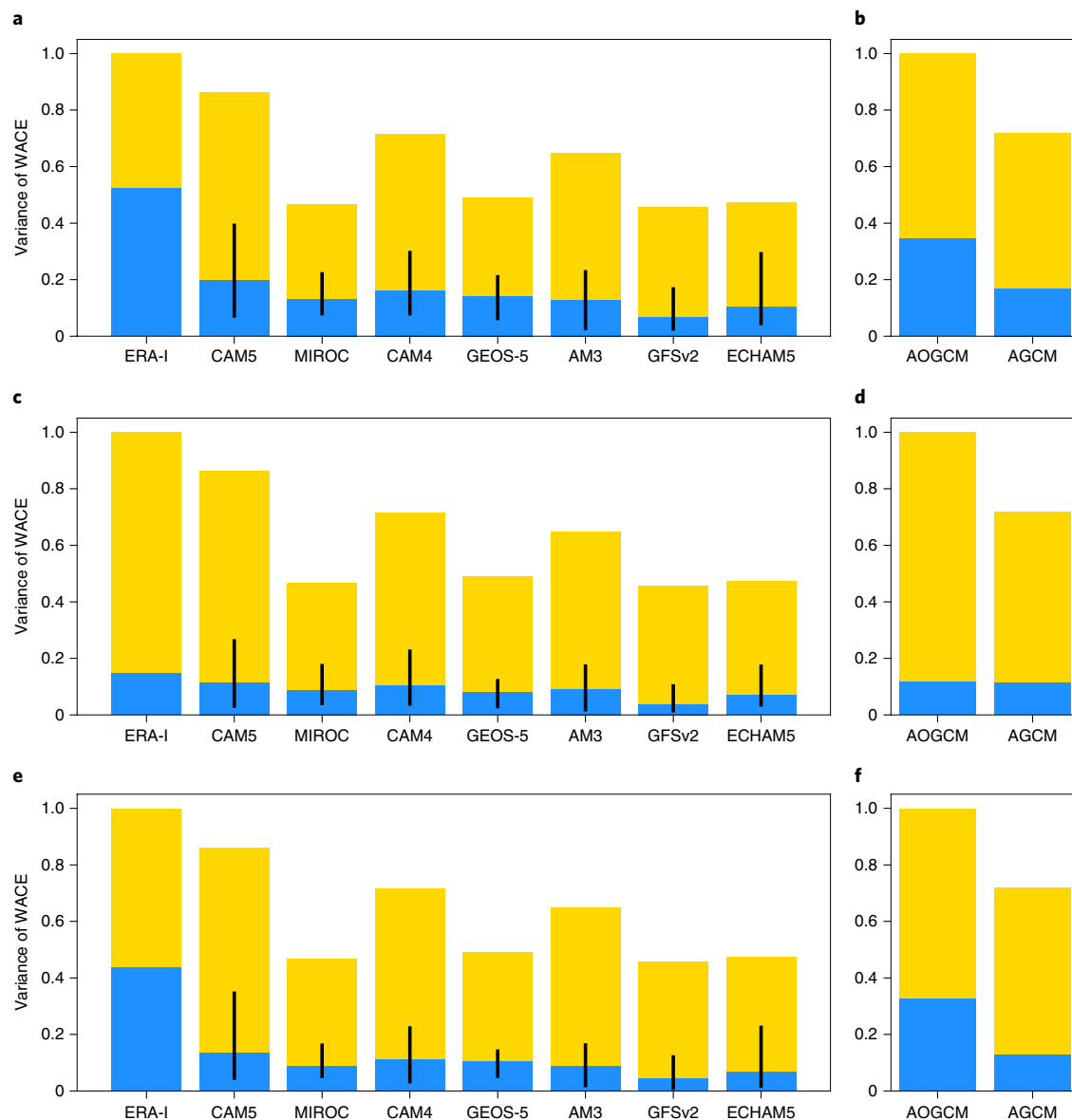


Fig. 1 | Observed and modelled estimates of the total and sea-ice-driven WACE variance. a, Total variance of WACE for ERA-Interim (ERA-I) and seven AGCM experiments. The y axis in **a** is scaled by the total WACE variance in ERA-I. The blue bars show the variance explained by Barents-Kara sea ice estimated from $r^2\sigma^2$. For the AGCMs, the bars show results for all ensemble members (concatenated in series) and the vertical black lines provide the ensemble ranges. **b,** Same as **a** but for a single AGCM (CAM5) and its parent AOGCM (CESM-CAM5). The y axis in **b** is scaled by the total WACE variance in the coupled model. **c,d,** Same as **a,b**, but calculating $r^2\sigma^2$ with Barents-Kara sea ice one month ahead of the WACE. **e,f,** Same as **a,b**, but calculating $r^2\sigma^2$ with Barents-Kara sea ice one month behind the WACE.

and is physically justified here because the upward surface heat flux anomalies that might cause or reinforce the WACE pattern tend to lag reductions in Barents-Kara sea ice^{5,11}. Conversely, WACE-induced (and more generally, circulation-induced) downward heat flux anomalies tend to precede reductions in Barents-Kara sea ice^{5,11}. Blackport et al.⁵ presented evidence that this one-month lead or one-month lag approach can effectively distinguish between regimes of ‘ice driving atmosphere’ and ‘atmosphere driving ice’. To test our hypothesis, we repeated the analysis, but calculated $r^2\sigma^2$ with Barents-Kara sea ice one month ahead of the WACE pattern (see Methods). The AOGCM and AGCM gave almost identical estimates of the WACE variance driven by sea ice when using the refined method (Fig. 1d), lending support to our hypothesis and suggesting that ocean coupling has little effect on the WACE response to sea-ice loss.

Applying the refined approach to the observations and AGCMs (Fig. 1c) leads to a different conclusion on model performance to that in Mori et al.¹. Now, the estimates from all seven AGCMs lie close to observation-based estimates. Only two AGCMs have ensemble member ranges that do not span the observed estimate, and only by very small margins (probably within observational uncertainty, which has not been accounted for here). We conclude that the modelled and observed estimates of the WACE variance driven by sea ice are consistent with each other. This suggests that AGCMs are able to realistically simulate the WACE response to sea-ice loss, effectively ruling out either AGCM error or a lack of ocean coupling as the main reason for the stronger Eurasian cooling trends in observations than in AGCMs.

We next repeated the analysis and calculated $r^2\sigma^2$ with Barents-Kara sea ice lagging one month behind the WACE pattern. The $r^2\sigma^2$

value now provides an estimate of the WACE variance related to atmospheric driving of sea ice. The $r^2\sigma^2$ value is non-zero in the AGCMs partly because the imprint of observed WACE variability is contained in the sea-ice conditions specified in the AGCMs. Also, due to serial correlation, the sum of the $r^2\sigma^2$ at one-month lead (Fig. 1d,e) and one-month lag (Fig. 1c,d) does not, and should not be expected to equal the contemporaneous $r^2\sigma^2$ (Fig. 1a,b). Nevertheless, when sea ice lags the WACE pattern, we find a clear discrepancy between observations and AGCMs (Fig. 1e) and between the AOGCM and AGCM (Fig. 1f), in stark contrast to the consistency found when sea ice leads the WACE (Fig. 1c,d). This provides further evidence that the apparent divergence between observations and models reported by Mori et al.¹ stems from the inability of AGCM experiments to simulate the effects of the WACE on sea ice, and the failure of the original $r^2\sigma^2$ method to extract the sea-ice-driven fraction of observed WACE variability. This reasoning is probably valid across timescales, at least qualitatively, given that WACE-related weather patterns drive warming in the Arctic (thereby reducing sea ice) on sub-monthly^{5,11–13}, monthly^{5,14,15}, seasonal^{5,16} and multidecadal^{2–5,7,17} timescales.

In summary, here we have shown that the two main conclusions of Mori et al.¹—that models systematically underestimate Eurasian cooling in response to Arctic sea-ice loss and that ~44% of observed Eurasian cooling is attributable to sea-ice loss—were based on a misleading comparison of observations and models. When fair comparisons are made, observations and models agree on the fraction of WACE variance driven by sea ice. There is, therefore, no justification for the adjustment to the model output that leads Mori et al.¹ to conclude that 32–51% of observed Eurasian winter cooling from 1995–2014 is attributable to sea-ice loss. Without this misleading adjustment, models suggest that sea-ice loss has contributed little to colder Eurasian winters, which can instead be largely explained as a manifestation of internal climate variability^{2–5}.

Online content

Any methods, additional references, Nature Research reporting summaries, source data, extended data, supplementary information, acknowledgements, peer review information; details of author contributions and competing interests; and statements of data and code availability are available at <https://doi.org/10.1038/s41558-019-0635-1>.

Received: 27 March 2019; Accepted: 18 October 2019;
Published online: 26 November 2019

References

1. Mori, M., Kosaka, Y., Watanabe, M., Nakamura, H. & Kimoto, M. A reconciled estimate of the influence of Arctic sea-ice loss on recent Eurasian cooling. *Nat. Clim. Change* **9**, 123–129 (2019).
2. McCusker, K. E., Fyfe, J. C. & Sigmond, M. Twenty-five winters of unexpected Eurasian cooling unlikely due to Arctic sea-ice loss. *Nat. Geosci.* **9**, 838–842 (2016).
3. Sun, L., Perlwitz, J. & Hoerling, M. What caused the recent “Warm Arctic, Cold Continents” trend pattern in winter temperatures? *Geophys. Res. Lett.* **43**, 5345–5352 (2016).

4. Ogawa, F. et al. Evaluating impacts of recent Arctic sea ice loss on the northern hemisphere winter climate change. *Geophys. Res. Lett.* **45**, 3255–3263 (2018).
5. Blackport, R., Screen, J., van der Wiel, K. & Bintanja, R. Minimal influence of reduced Arctic sea ice on coincident cold winters in mid-latitudes. *Nat. Clim. Change* **9**, 697–704 (2019).
6. Deser, C., Sun, L., Tomas, R. A. & Screen, J. Does ocean coupling matter for the northern extratropical response to projected Arctic sea ice loss? *Geophys. Res. Lett.* **43**, 2149–2157 (2016).
7. Smith, D., Dunstone, N., Scaife, A., Fiedler, E., Copsey, D. & Hardiman, S. Atmospheric response to Arctic and Antarctic sea ice: the importance of ocean-atmosphere coupling and the background state. *J. Clim.* **30**, 4547–4565 (2017).
8. Collow, T., Wang, W. & Kumar, A. Simulations of Eurasian winter temperature trends in coupled and uncoupled CFSv2. *Adv. Atmos. Sci.* **35**, 14–26 (2018).
9. Sun, L., Alexander, M. & Deser, C. Evolution of the global coupled climate response to Arctic sea ice loss during 1990–2090 and its contribution to climate change. *J. Clim.* **31**, 7823–7843 (2018).
10. Screen, J. et al. Consistency and discrepancy in the atmospheric response to Arctic sea-ice loss across climate models. *Nat. Geosci.* **11**, 153–163 (2018).
11. Sorokina, S. A., Li, C., Wettstein, J. J. & Kvamstø, N. G. Observed atmospheric coupling between Barents Sea ice and the warm-Arctic cold-Siberian anomaly pattern. *J. Clim.* **29**, 495–511 (2016).
12. McGraw, M. & Barnes, E. New insights on subseasonal Arctic-midlatitude causal connections from a regularized regression model. *J. Clim.* <https://doi.org/10.1175/JCLI-D-19-0142.1> (2019).
13. Gong, T. & Luo, D. Ural blocking as an amplifier of the Arctic sea ice decline in winter. *J. Clim.* **30**, 2639–2654 (2017).
14. Sato, K., Inoue, J. & Watanabe, M. Influence of the Gulf Stream on the Barents Sea ice retreat and Eurasian coldness during early winter. *Environ. Res. Lett.* **9**, 084009 (2014).
15. Peings, Y. Ural blocking as a driver of early-winter stratospheric warmings. *Geophys. Res. Lett.* **46**, 5460–5468 (2019).
16. Kelleher, M. & Screen, J. Atmospheric precursors of and response to anomalous Arctic sea ice in CMIP5 models. *Adv. Atmos. Sci.* **35**, 27–37 (2018).
17. Sung, M., Kim, S., Kim, B. & Choi, Y. Interdecadal variability of the warm Arctic and cold Eurasia patterns and its North Atlantic origin. *J. Clim.* **31**, 5793–5810 (2018).

Acknowledgements

The authors thank M. Mori for providing data from the MIROC simulations and for useful discussions. We acknowledge the individuals and modelling groups that contributed to the Facility for Climate Assessments (FACTS) multimodel dataset and the CESM Large Ensemble Project.

Author contributions

J.A.S. and R.B. jointly conceived the analysis. R.B. created Fig. 1. J.A.S. wrote the manuscript with input from R.B.

Competing interests

The authors declare no competing interests.

Additional information

Correspondence and requests for materials should be addressed to J.A.S.

Peer review information *Nature Climate Change* thanks Hans Chen, Yannick Peings and Qihong Tang for their contribution to the peer review of this work.

Reprints and permissions information is available at www.nature.com/reprints.

Publisher's note Springer Nature remains neutral with regard to jurisdictional claims in published maps and institutional affiliations.

© The Author(s), under exclusive licence to Springer Nature Limited 2019

Methods

In Fig. 1a,c,e, we use the exact same data as Mori et al.¹. Briefly, observational results come from the ERA-Interim reanalysis for the period 1979–2014 and modelled results come from seven AGCM simulations in which observed sea surface temperatures and sea ice have been specified. Further details on these model simulations can be found in Mori et al.¹. In Fig. 1b,d,f, we also analyse two experiments performed as part of the Community Earth System Model (CESM) Large Ensemble project¹⁸. The first is a 200-year section (years 401–600) of a pre-industrial control run of the CESM configured with the Community Atmosphere Model version 5 (CAM5). CESM–CAM5 is a global coupled climate model with a horizontal resolution of approximately 1° in all model components. The second additional experiment is a 200-year simulation with CAM5 in which sea surface temperatures and sea ice were specified from years 401–600 of the parent CESM–CAM5 simulation. External forcing is the same in both simulations. Initially in Fig. 1a, we employed the same methodologies as Mori et al.¹ to calculate the WACE pattern, the WACE time series and the Barents–Kara sea-ice index (see Mori et al.¹ for details), with one exception. We computed the WACE and Barents–Kara sea-ice time series from monthly averages, whereas Mori et al.¹ used winter averages. The purpose of this modification is to facilitate subseasonal lead–lag correlations. Projecting near-surface temperatures for December, January and February separately onto the winter mean WACE pattern produced monthly WACE time series. Figure 1a shows the total and sea-ice-driven variance for the three winter months combined. To construct Fig. 1b, we performed an analogous analysis but substituted data from ERA-Interim with that from CESM–CAM5. More specifically, we derived the WACE pattern as the leading mode of covariability from singular value decomposition applied to the CESM–CAM5 and CAM5 simulations. The r^2 value was then calculated by correlating the corresponding WACE time series with the Barents–Kara sea-ice index from CESM–CAM5. In this so-called perfect model comparison^{19,20},

the coupled model simulation is an analogue for the observations and any difference between the CESM–CAM5 and CAM5 results can therefore be attributed solely to ocean coupling. To construct Fig. 1c–f, we adapted the approach used by Mori et al.¹ by introducing a one-month lead or lag time between the WACE and Barents–Kara sea-ice time series. In Fig. 1c,d, we show the combination of three cases where the Barents–Kara sea-ice index leads the WACE time series by one month: November sea ice correlated with December WACE, December sea ice correlated with January WACE and January sea ice correlated with February WACE. In Fig. 1e,f, we show the combination of three cases where the Barents–Kara sea-ice index lags the WACE time series by one month: January sea ice correlated with December WACE, February sea ice correlated with January WACE and March sea ice correlated with February WACE.

Data availability

The FACTS and CESM simulations are freely available and were obtained from the following repositories: <https://www.esrl.noaa.gov/psd/repository/facts> and <https://www.cesm.ucar.edu/projects/community-projects/LENS/>.

References

18. Kay, J. E. et al. The Community Earth System Model (CESM) large ensemble project: a community resource for studying climate change in the presence of internal climate variability. *Bull. Am. Meteorol. Soc.* **96**, 1333–1349 (2015).
19. Chen, H. & Schneider, E. K. Comparison of the SST-forced responses between coupled and uncoupled climate simulations. *J. Clim.* **27**, 740–756 (2014).
20. Zhou, Z., Xie, S., Zhang, G. J. & Zhou, W. Evaluating AMIP skill in simulating interannual variability over the Indo–Western Pacific. *J. Clim.* **31**, 2253–2265 (2018).